

This is the peer reviewed version of the following article: Xu, W., Huang, L. -, Wong, M. -, Chen, L., Bai, G., & Hao, J. (2017). Environmentally friendly hydrogel-based triboelectric nanogenerators for versatile energy harvesting and self-powered sensors. *Advanced Energy Materials*, 7(1), 1601529, which has been published in final form at <https://doi.org/10.1002/aenm.201601529>. This article may be used for non-commercial purposes in accordance with Wiley Terms and Conditions for Use of Self-Archived Versions. This article may not be enhanced, enriched or otherwise transformed into a derivative work, without express permission from Wiley or by statutory rights under applicable legislation. Copyright notices must not be removed, obscured or modified. The article must be linked to Wiley's version of record on Wiley Online Library and any embedding, framing or otherwise making available the article or pages thereof by third parties from platforms, services and websites other than Wiley Online Library must be prohibited.

Environmentally Friendly Hydrogel-based Triboelectric Nanogenerators for Versatile Energy Harvesting and Self-Powered Sensors

Wei Xu^{a/}, Long-Biao Huang^{a,c/}, Man-Chung Wong^{a,b}, Li Chen^{a,b}, Gongxun Bai^{a,b}, Jianhua Hao^{a,b,}*

W. Xu, L. B. Huang, W. C. Wong, L. Chen, G. X. Bai, Prof. J. H. Hao,
Department of Applied Physics, The Hong Kong Polytechnic University, Hong Kong, China
E-mail: jh.hao@polyu.edu.hk

W. C. Wong, L. Chen, G. X. Bai, Prof. J. H. Hao,
The Hong Kong Polytechnic University Shenzhen Research Institute, Shenzhen 518057,
China

Dr. L. B. Huang
Department of Applied Chemistry, Northwestern Polytechnical University, Xi'an Shaanxi
710072, China

Keywords: triboelectric nanogenerators, environmentally friendly, hydrogel, flexible, self-powered sensors

Abstract:

Triboelectric nanogenerators (TENGs) as a promising energy harvesting technology have been rapidly developed in recent years. However, the research based on fully flexible and environmentally friendly TENGs is still limited. Herein, we demonstrate, for the first time, a hydrogel-based triboelectric nanogenerator (Hydrogel-TENG) with high flexibility, **recyclability** and environmental friendliness simultaneously. The standard Hydrogel-TENG can generate a maximum output power of 2 mW at a load resistance of 10 Mn. The tube-shaped Hydrogel-TENG can harvest mechanical energy from various human motions, including bending, twisting and stretching. Furthermore, the system can serve as self-powered sensors to detect the human motions. Additionally, the utilized Polyvinyl Alcohol (PVA) hydrogel employed in this study is recyclable to benefit for fabricating the renewable TENG. The open-circuit voltage of renewed hydrogel-TENG can reach up to 92% of the pristine output voltage. This research will pave a potential approach for the development of flexible energy sources and self-powered motion sensors in environmentally friendly way.

1. Introduction

As an emerging electronics with excellent deformability and reliability, the flexible electronics is attracting extensive interest, enabling various applications in wearable devices, epidermal electronics and bendable display etc.¹⁻⁵ Meanwhile, the massive applications of these modern electronics inevitably causes environment issues due to their non-degradability in the environment. As a solution, green electronics with high biodegradability and biocompatibility has emerged with growing focus.⁶⁻⁸ The advance in flexible electronics and green electronics put forward severe challenges on the traditional power source.⁹⁻¹¹ In this regards, developing sustainable, flexible and environmentally friendly power generation devices is highly desired to drive these emerging electronics and deserves more attempts.^{12, 13}

Recently, triboelectric nanogenerators (TENGs) as a sustainable power source have been achieving rapid progress from both academia and industry.¹⁴⁻¹⁶ Based on the conjunction of triboelectrification and electrostatic induction, TENGs can efficiently convert ambient mechanical energies into electricity with simple fabrication process and expected sizes.^{3, 16-18} Most importantly, TENGs can be designed and fabricated with flexibility, elasticity, biodegradation and bio-compatibility through the choice of constituent materials,^{3, 8, 14} and therefore they becomes promising candidates to drive flexible electronics and green electronics. Nowadays, considerable efforts have been contributed to develop flexible TENGs,¹⁹⁻²³ such as fiber-based TENG, rubber-based TENG, TENG coat and TENG based on conductive liquid. Compared with the rigid TENGs, flexible TENGs can harvest ambient mechanical energy in various modes and thus gain continuous concern from relevant industries.^{5, 20} Accompanying with the widespread applications of flexible TENGs in the new-generation electronics, it is highly necessary to develop novel TENGs with high flexibility and environmental friendliness simultaneously to meet dual demand of both flexible electronics and green electronics. To our knowledge, very limited research has been reported in the related field.²⁴

Hydrogel, an environmentally friendly material with 3D crosslinking network of polymer

1 chains,²⁵⁻²⁷ could be an ideal material to realize flexible and environmentally friendly TENGs.
2 The 3D network structure of hydrogel leads to excellent mechanical properties, including high
3 softness, flexibility and elasticity.²⁶⁻²⁹ In addition, the hydrogel also remains excellent properties
4 of environmental friendly, such as biodegradability and biocompatibility.^{25, 27, 30} These
5 advantages may result in the extensive applications of hydrogel in flexible electronics and green
6 electronics.²⁹⁻³¹ Although some attempts have been made in innovating hydrogel-based
7 electronics for energy storage and conversion applications,³¹⁻³⁴ there has been no report on
8 applying hydrogel to TENGs.
9

10
11
12
13
14
15
16
17
18
19 Herein, we presented a novel hydrogel-based triboelectric nanogenerator (Hydrogel-
20 TENG) with full flexibility and environmental friendliness by using physical-crosslinking
21 Polyvinyl Alcohol (PVA) hydrogel as substrate materials. For the standard Hydrogel-TENG
22 which consists of a polydimethylsiloxane (PDMS) film attached on hemispheric-shaped
23 hydrogel and an aluminum foil, a peak output power of 2 mW can be achieved at a load
24 resistance of 10 Mn. The tube-shaped Hydrogel-TENG can harvest mechanical energy from
25 various human motions, including bending, twisting and stretching, and serve as self-powered
26 human motion sensor. Besides, the utilized PVA hydrogel with biodegradability and
27 biocompatibility presents the recyclability, which provides the Hydrogel-TENG with
28 advantages of environmental friendliness and low-cost.
29
30
31
32
33
34
35
36
37
38
39
40
41
42
43
44
45
46

47 **2. Results and discussions**

48 As shown in **Figure 1a**, the structure of Hydrogel-TENG consists of two parts: the top
49 contact layer with hemispheric shape and the bottom contact layer with flat structure. For the
50 top contact layer, a hemisphere-shaped PVA hydrogel with a nickel fabric electrode was
51 encapsulated by a PDMS film. Due to the high elasticity of PVA hydrogel and PDMS film, the
52 top contact layer shows excellent expansibility, flexibility and stretchability under the stimuli
53 of external force. The bottom contact layer is an Al foil attached on the surface of hydrogel
54
55
56
57
58
59
60
61
62
63
64
65

1 substrate. The Al foil with anodized nanostructure plays dual roles as triboelectric contact
2 material and electrode, and its morphology is shown in **Figure 1b**. As mentioned in literatures,¹⁹
3 the nanostructures on the surface of Al foil could enhance the performance of TENGs by
4 increasing the effective contact area.
5
6
7

8
9 The operation mechanism of the Hydrogel-TENG is schematically illustrated in **Figure**
10 **1c-1f**. When a pressure force is applied to Hydrogel-TENG, the PDMS film and Al foil are
11 adequately contacted due to the elastic expansion of the hydrogel and PDMS film, wherein the
12 maximum contact area (A_{max}) between PDMS film and nano-patterned Al electrode is achieved
13 (**Figure 1c**). Since the surface electron affinity of PDMS is higher than Al,³⁵ electrons will be
14 transferred at the interface between Al foil and PDMS, leaving positive triboelectric charges on
15 the Al foil surface and corresponding negative triboelectric charges on the PDMS surface. By
16 releasing the external force (**Figure 1d**), PDMS film and nano-patterned Al electrode could be
17 separated due to the elastic contraction of the expanded hydrogel and PDMS film, which leads
18 to the decrement of contact area. **Accompanying with the electrostatic induction between**
19 **PDMS and Ni electrode**, the separation of charged contact surfaces creates the electric potential
20 difference between Ni and Al electrodes, which drives electrons flow from the Ni electrode to
21 the Al electrode until the external force is fully released (**Figure 1f**), where the minimum
22 contact area (A_{min}) is reached. When the Hydrogel-TENG is compressed again (**Figure 1e**), an
23 opposite electric potential difference will be formed, which causes the electrons flow back to
24 the Ni electrode from the Al electrode until the A_{max} is achieved again (**Figure 1c**). Therefore,
25 the AC electricity can be continuously generated by periodical contact-separation between
26 PDMS film and Al electrode. **The electric output amplitude** depends on the change of contact
27 area (LIA), which equals to $A_{max} - A_{min}$.
28
29
30
31
32
33
34
35
36
37
38
39
40
41
42
43
44
45
46
47
48
49
50
51
52
53

54 In order to characterize the electric output of Hydrogel-TENG, a standard device with the
55 bottom contact layer of 8 cm x 8 cm was fabricated by fixing the frozen time of PVA (5.5 hours),
56 the concentration of PVA aqueous solution (25 %) and the diameter of hemisphere hydrogel (4
57
58
59
60
61
62
63
64
65

cm). As shown in **Figure 2a-2b**, the open-circuit voltage and short-circuit current of standard device could achieve up to 200 V and 22.5 μ A, respectively. Besides, the short-circuit transfer charge (Q_{sc}) of the device is also shown in **Figure S1a**. For further evaluating performance of the Hydrogel-TENG, the resistance dependence of the output voltage and current is investigated as illustrated in **Figure 2c**. The results reveal that the voltage increases with increment of loading resistance, while the current shows a reverse trend. Correspondingly, the maximum electric power could reach up to 2 mW at a load resistance of around 10 M Ω as shown in **Figure S2**. The as-prepared TENG can light up 20 commercial white LEDs simultaneously as displayed in **Figure 2d**.

As aforementioned, the AC triboelectricity is generated by periodical change of the contact area between PDMS film and Al foil, which is caused by elastic deformation of the hydrogel. It means that the elasticity of hydrogel has an effect on the performance of the Hydrogel-TENG. Herein, there are two parameters which can affect the elasticity of PVA hydrogel, i.e. frozen time and concentration of PVA. **Figure 3a** and **3b** show the relationship between the frozen time and the performance of Hydrogel-TENG. The results indicate that the maximum open-circuit voltage of 200 V and the maximum short-circuit of 22.5 μ A are achieved at the frozen time of 5.5 hrs. Further elongating and shorting the frozen time leads to the decrement of open-circuit voltage and short-circuit current. This is mainly attributed to the elasticity change of hydrogel under different fabrication conditions. The elasticity of utilized hydrogel originates from the formation of micro-crystallites among PVA molecular chains. These micro-crystallites can serve as physical crosslinkers and provides the hydrogel with 3D crosslinking network structure and the tunable elasticity.³⁶⁻³⁸ When extending the frozen time for 5.5 hrs, the size and amount of micro-crystallites increase and the expansibility of PVA hydrogel thus decreases, which leads to the reduced *LIA*. Therefore, the open-circuit voltage and short-circuit current decrease to about 165 V and 18 μ A, respectively at the frozen time of 7.5 hrs. However, when the frozen time is less than 5.5 hrs, the amount of micro-crystallites existed in PVA hydrogel is

1 limited with low crosslinking density in 3D crosslinking network. Accordingly, the hydrogel
2 cannot provide sufficient resilience force to separate the charged contact surfaces completely
3 after the external force is released. Hence, the electric output is decreased. **Figure 3c** and **3d**
4 present the performance of Hydrogel-TENG fabricated with PVA aqueous solution at different
5 concentration. When the concentration of PVA changes from 25 % to 17.5 %, the open-circuit
6 voltage and short-circuit current decrease from 200 V to 171 V and from 22.5 μA to 20.7 μA ,
7 respectively. At the low PVA concentration, the reduced amount of PVA molecules will limit
8 the formation of micro-crystallites, which leads to the lower resilience of the hydrogel. As a
9 result, the charged contact surfaces cannot be separated effectively and results in the reduced
10 electric output of Hydrogel-TENG. Further reducing the concentration of PVA, the hydrogel
11 has not enough micro-crystallites to remain hemispheric structure even at the original state. We
12 further investigate the dependence of electric output on the diameter of hemisphere-shaped
13 hydrogel as shown in **Figure 3e** and **3f**. The results indicate that the open-circuit voltage
14 increases obviously from 105 V to 236 V when the diameter of hydrogel increases from 2 cm
15 to 5 cm. The electric output of Hydrogel-TENGs mainly originates from the change of contact
16 area (LIA) between triboelectric materials, which is related to the change of the average
17 separation distance between contact layers (Lld). According to earlier model^{39, 40, 41} as illustrated
18 in supporting information, the open-circuit voltage of TENGs could be approximately
19 calculated as

$$V_{oc} = \frac{at1d}{E_0}$$

20 where V_{oc} is the open-circuit voltage, c_0 is the permittivity of vacuum, a is the average surface
21 charge density of contact materials, Lld is the change of the average separation distance between
22 the top contact layer and the bottom contact layer. Under a certain external force, increasing the
23 diameter of hydrogel could cause the increase of Lld , thereby leading to the increment of LIA
24 and electric output. When the diameter of hydrogel arrives at 5 cm, the saturation of the electric
25

1 output is occurred. The possible reason behind the observation is that *LIA* already reaches the
2 maximum value based on the certain applied external force and the electric output will not
3 enhance when increasing the diameters. For further comparing the quality of devices with
4 different parameters, their Q_{sc} and performance Figure-of-merit (FOMp)⁴¹ are shown in Figure
5 S1b-d and Table S1, respectively.
6
7
8
9

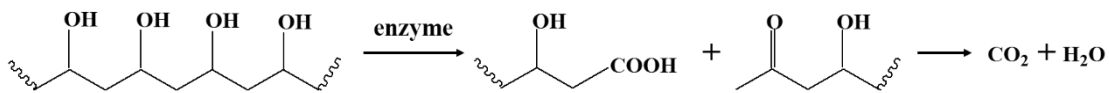
10 For harvesting mechanical energy from various human motions, a Hydrogel-TENG with
11 tube-shaped structure is designed by combining several standard devices as shown in Figure
12 4a. The system includes six series connected hemisphere-shaped top contact layers with the
13 diameter of 2.5 cm, and a tube-shaped bottom contact layer (8 cm x 10 cm). Under the external
14 force, the tube-shaped Hydrogel-TENG can deform and cause the volume compress. This leads
15 to the change of the contact area between PDMS and nano-patterned Al electrode, and therefore
16 results in the generation of triboelectricity. Due to the high deformation and flexibility of
17 hydrogel, the tube-shaped Hydrogel-TENG shows great flexibility and is able to deform
18 following various human motions as demonstrated in Figure S3. The open-circuit voltages of
19 tube-shaped Hydrogel-TENG generated from bending, twisting and stretching motion are
20 shown in Figure 4b, 4c and 4d, respectively. The results indicate that the Hydrogel-TENG
21 could harvest mechanical energy from different human motions and the open-circuit voltage
22 can reach up to about 40 V when the bending angle and twisting angle are 150°. Additionally,
23 it is also observed that the open-circuit voltage of Hydrogel-TENG is enhanced with the
24 increment of bending angle, twisting angle and tensile stain as shown in Figure 4b, 4c and 4d.
25 That is contributed to the larger *LIA* with the increased deformation of the TENGs, which leads
26 to the improved electric output.
27
28
29
30
31
32
33
34
35
36
37
38
39
40
41
42
43
44
45
46
47
48
49
50
51

52 Based on above results, the as-prepared Hydrogel-TENG could generate distinctive
53 voltage signals triggered by various motions, which indicates its potential applications as a self-
54 powered sensor to monitor the human motion in real time. Fig Sa-Sd exhibit the application of
55 the Hydrogel-TENG as a self-powered elbow-joint motion sensor, which is a tube-shaped
56
57
58
59
60
61
62
63
64
65

Hydrogel-TENG with the diameter of 1 cm and the length of 18 cm. The device is fixed over the straighten elbow joint at the original state. After changing the bending angle periodically, including 30°, 90° and 120°, the different output voltages of 3.5 V, 13 V and 16 V are generated, respectively (**Figure Sa**). Correspondingly, the relationship between open-circuit voltage and the bending angle is shown in **Figure Sc**. The results presents that the bending angle is proportional to the open-circuit voltage of the Hydrogel-TENG at the bending rate of 1.5 times/s. Hence, the change of bending angle in the elbow joint motion can be monitored through the change of open-circuit voltage. Moreover, the Hydrogel-TENG is also capable of distinguishing elbow motions with different bending rate by monitoring the peak interval and peak amplitude of open-circuit voltage. As shown in **Figure Sb**, when the bending rate of elbow joint is increased from 0.6 times/s to 2 times/s, the peak interval is shortened from 1.67 s to 0.5 s with the increased voltage amplitude from 3.7 V to 17.5 V. **Figure Sd** shows the dependence of peak interval and open-circuit voltage on the bending rate with the bending angle of 90°. It is observed that the peak interval between adjacent voltage signals is inversely proportional to the bending rate, while the open-circuit voltage is linearly associated with the bending rate, which indicates the advantages of hydrogel-TENGs as a bending rate sensor. By adjusting the dimension of device, the Hydrogel-TENG could also be utilized to detect human motion in other human body parts. **Figure S4** presents a finger-joint motion sensor based on a small size of tube-shaped Hydrogel-TENG with the diameter of 1 cm and length of 8 cm. It shows that the difference in bending angle of finger joint could also be recognized by measuring the open-circuit voltage. Improving bending angle from 30° to 120° leads to the similar increment in open-circuit voltage from 2.7 V to 5.1 V. Therefore, the as-prepared Hydrogel-TENG may identity different human motions by analyzing the peak amplitude and peak interval of voltage signals. In general, electronics which directly contact with human body has some specific requirements, such as non-toxicity, high comfortability, biocompatibility or biodegradability. In this context, the Hydrogel-TENG as a human motion sensor presents great advantages

1 compared with other flexible TENGs due to its high safety, biocompatibility and flexibility,
2 which might indicate its potential in diverse applications, such as artificial skin, health care,
3 wearable electronics and criminal investigation.
4
5

6
7 With the rapid development of modern electronics, the relevant environmental issues have
8 been raised due to the electronic wastes pollution. As a kind of environmentally friendly
9 material, the PVA shows promising potential in the fabrication of green electronics with
10 biodegradability and biocompatibility to solve above problems.^{42, 43} The biodegradable reaction
11 of PVA in the environment is shown below:^{42, 43}
12
13
14
15
16
17



It should be mentioned that the final degradation products of PVA are carbon dioxide and water, which are highly safe for environment. Besides, other materials utilized in Hydrogel-TENG also present environmental compatibility. Briefly, PDMS is known polymer routinely utilized as a biomedical implant material and for cellular studies, while Al and Ni show abundant applications in various fields, such as metal implants and biomaterials.^{44, 45}

Therefore, the Hydrogel-TENG fabricated with PVA possesses excellent environmental friendliness. Additionally, the formation of micro-crystallites in the PVA hydrogel presents reversibility,³⁶⁻³⁸ which means that the 3D crosslinking network structure among PVA molecular chains could disappear with the melting of micro-crystallites at high temperature and rebuild with the regeneration of micro-crystallites under the frozen treatment. Based on this process, the PVA hydrogel utilized in the Hydrogel-TENG can be fully recycled for the refabrication of device without environmental contamination. To provide further evidence, the optical images in **Figure 6a** show the recycling process of PVA hydrogel. The pristine hemisphere-shaped hydrogel with the diameter of 4cm is firstly prepared by freezing 25% PVA aqueous solution at - 20 C for 5.5 hrs, where the micro-crystallites among PVA molecular chains are generated (i). Then the hydrogel is cut into pieces (ii). After heating the

1 hydrogel pieces for 1 hr at 95 °C, a PVA aqueous solution is achieved due to the
2 disappearance of micro-crystallites at high temperature (iii). By means of the frozen-thawed
3 process of PVA aqueous solution at - 20 C for 5.5 hrs,³⁶⁻³⁷ the 3D crosslinking network
4 structure can be re-built with the regeneration of micro-crystallites, which leads to the
5 formation of hemisphere-shaped hydrogel (iv) for the refabrication of Hydrogel-TENG.
6
7
8
9
10
11 **Figure 6b** and **6c** show the open-circuit voltages of the pristine Hydrogel-TENG and the
12 refabricated Hydrogel-TENG, respectively. Compared with the voltage of 200 V generated by
13 the pristine device (**Figure 6b**), the voltage of the refabricated device can arrive at about 185
14 V (**Figure 6c**), which is about 92 % as high as that of the pristine one. This demonstrates the
15 recyclability of the Hydrogel-TENG as a mechanical energy harvester, and also provides a
16 feasible way for developing environmentally friendly and low-cost electronics.
17
18
19
20
21
22
23
24
25
26

27 **3. Conclusion**

28
29 In summary, a high-flexible, environmentally friendly and recyclable Hydrogel-TENG is
30 demonstrated for harvesting ambient mechanical energy and serving as self-powered human
31 motion sensors. The dependence of electric outputs on the frozen time, the concentration of
32 PVA and the dimension of standard device has been systematically investigated. The standard
33 device can generate an open-circuit voltage of 200 V and a short-circuit current of 22.5 μ A
34 with the peak power of approximately 2 mW at a load resistance of 10 Mn and therefore
35 power 20 LEDs directly. The tube-shaped Hydrogel-TENG is capable of harvesting
36 mechanical energies from various kind of motions, including bending, twisting and stretching.
37
38 It can also serve as self-powered human motion sensor. Moreover, the utilized PVA hydrogel
39 is recyclable for fabricating renewable Hydrogel-TENG. This study provides the feasibility of
40 developing flexible, environmentally friendly and recyclable power generation devices as well
41 as self-powered sensors based on the hydrogel.
42
43
44
45
46
47
48
49
50
51
52
53
54
55
56
57
58
59
60

61 **4. Experimental Section**

1
2
3
4
5
6
7
8
9
10
11
12
13
14
15
16
17
18
19
20
21
22
23
24
25
26
27
28
29
30
31
32
33
34
35
36
37
38
39
40
41
42
43
44
45
46
47
48
49
50
51
52
53
54
55
56
57
58
59
60
61
62
63
64
65

Fabrieation of the standard Hydrogel-TENG: (1) Fabrication of the top contact layer: To achieve a hemisphere-structured PVA hydrogel, the PVA 1799 aqueous solution with the concentration of 17.5 %, 20 % and 25 % were firstly poured into a hemispheric PMMA vessel under 80 C, a circular nickle fabric was inserted into the PVA aqueous solution as electrode. Then the whole set was frozen at - 20 C for 3.5 - 7.5 hrs, and thawed consequently for 2 hrs to form the hemisphere-structured hydrogel. Then, the hydrogel was encapsulated by PDMS thin film which was fabricated by curing the mixture of PDMS and cross-linker (Sylgard 184, Dow Corning) at 80 °C for 1 hr in an oven. The ratio of PDMS to crosslinker is 30:1. (2) Fabrication of the bottom contact layer: The nanoporous structure on the aluminium surface was fabricated as following steps: An Al foil was used as anode and put into 3 % (mass fraction) oxalic acid ($H_2C_2O_4$) electrolyte for anodization of 5 hrs under a bias voltage of 30 V, with a platinum plate as the cathode. Then, the obtained Al layer was etched away in a chromic acid solution (20 g L^{-1}) at 60 °C for 2 hrs. Finally, the nanopatterned Al foil was attached on the surface of hydrogel substrate (8 cm x 8 cm). (3) The standard Hydrogel-TENG thus was achieved by assembling the top contact layer with the bottom contact layer. The optical image of the standard hydrogel-TENG is shown in **Figure SS** (supporting information).

Fabrieation of the tube-shaped Hydrogel-TENG: Six hemisphere-shaped top contact layers with the diameter of 2.5 cm are in series connection firstly. Then, the connected top contact layers are wrapped by a bottom contact layer (8 cm x 10 cm) to form the tube-shaped Hydrogel-TENG.

Measurement of the deviee: The open-circuit voltage and short-circuit current were measured by LeCroy WaveRunner Oscilloscope (44MXI) with the probe resistance value of 10 Mn and low noise current amplifier (Stanford Research Systems, SR570), respectively. An external force was applied by a linear mechanical motor. The surface morphology of the aluminum foil was characterized by a Hitachi SU-8010.

Supporting Information

Supporting Information is available from the Wiley Online Library or from the author.

Acknowledgements

W. X. and L.-B. H. contributed equally to this work. The research was financially supported by the grants from Research Grants Council of Hong Kong (GRF No. PolyU 153004/14P), PolyU Internal Grant (1-ZVGH), National Natural Science Foundation of China (Grant No. 11474241) and the Fundamental Research Funds for the Central Universities (3102015ZY067).

Received: ((will be filled in by the editorial staff))
Revised: ((will be filled in by the editorial staff))
Published online: ((will be filled in by the editorial staff))

Reference

- [1] D.-H. Kim, N. Lu, R. Ma, Y.-S. Kim, R.-H. Kim, S. Wang, J. Wu, S. M. Won, H. Tao, A. Islam, K. J. Yu, T.-i. Kim, R. Chowdhury, M. Ying, L. Xu, M. Li, H.-J. Chung, H. Keum, M. McCormick, P. Liu, Y.-W. Zhang, F. G. Omenetto, Y. Huang, T. Coleman and J. A. Rogers, *Science* **2011**, 333, 838.
- [2] R.-H. Kim, D.-H. Kim, J. Xiao, B. H. Kim, S.-I. Park, B. Panilaitis, R. Ghaffari, J. Yao, M. Li, Z. Liu, V. Malyarchuk, D. G. Kim, A.-P. Le, R. G. Nuzzo, D. L. Kaplan, F. G. Omenetto, Y. Huang, Z. Kang and J. A. Rogers, *Nat. Mater.* **2010**, 9, 929.
- [3] F. R. Fan, W. Tang and Z. L. Wang, *Adv. Mater.* **2016**, 28, 4283.
- [4] Y. Sun and J. A. Rogers, *Adv. Mater.* **2007**, 19, 1897.
- [5] C. Wu, X. Wang, L. Lin, H. Guo and Z. L. Wang, *ACS Nano* **2016**, 10, 4652.
- [6] Y. H. Jung, T.-H. Chang, H. Zhang, C. Yao, Q. Zheng, V. W. Yang, H. Mi, M. Kim, S. J. Cho, D.-W. Park, H. Jiang, J. Lee, Y. Qiu, W. Zhou, Z. Cai, S. Gong and Z. Ma, *Nat. Commun.* **2015**, 6, 7170.

- 1
2
3
4
5
6
7
8
9
10
11
12
13
14
15
16
17
18
19
20
21
22
23
24
25
26
27
28
29
30
31
32
33
34
35
36
37
38
39
40
41
42
43
44
45
46
47
48
49
50
51
52
53
54
55
56
57
58
59
60
61
62
63
64
65
- [7] M. Irimia-Vladu, *Chem. Soc. Rev.* **2014**, *43*, 6470.
- [8] Q. Zheng, Y. Zou, Y. Zhang, Z. Liu, B. Shi, X. Wang, Y. Jin, H. Ouyang, Z. Li and Z. L. Wang, *Sei. Adv.* **2016**, *2*, e1501478.
- [9] S. Niu, X. Wang, F. Yi, Y. S. Zhou and Z. L. Wang, *Nat. Commun.* **2015**, *6*, 8975.
- [10] Z. L. Wang, J. Chen and L. Lin, *Energy Environ. Sci.* **2015**, *8*, 2250.
- [11] Z. L. Wang, *Faraday Discuss.* **2014**, *J76*, 447.
- [12] H. Nishide and K. Oyaizu, *Science* **2008**, *3J9*, 737.
- [13] Z. Zhu, T. Kin Tam, F. Sun, C. You and Y. H. Percival Zhang, *Nat. Commun.* **2014**, *5*, 3026.
- [14] F.-R. Fan, Z.-Q. Tian and Z. L. Wang, *Nano Energy* **2012**, *J*, 328.
- [15] L.-B. Huang, G. Bai, M.-C. Wong, Z. Yang, W. Xu and J. Hao, *Adv. Mater.* **2016**, *28*, 2744.
- [16] G. Zhu, B. Peng, J. Chen, Q. Jing and Z. L. Wang, *Nano Energy* **2015**, *J4*, 126.
- [17] Z. L. Wang, *ACS Nano* **2013**, *7*, 9533.
- [18] H. Zhang, Y. Yang, Y. Su, J. Chen, C. Hu, Z. Wu, Y. Liu, C. P. Wong, Y. Bando and Z. L. Wang, *Nano Energy* **2013**, *2*, 693.
- [19] F. Yi, L. Lin, S. Niu, P. K. Yang, Z. Wang, J. Chen, Y. Zhou, Y. Zi, J. Wang, Q. Liao, Y. Zhang and Z. L. Wang, *Adv. Funct. Mater.* **2015**, *25*, 3688.
- [20] F. Yi, X. Wang, S. Niu, S. Li, Y. Yin, K. Dai, G. Zhang, L. Lin, Z. Wen, H. Guo, J. Wang, M.-H. Yeh, Y. Zi, Q. Liao, Z. You, Y. Zhang and Z. L. Wang, *Sei. Adv.* **2016**, *2*, e1501624.
- [21] X. Pu, L. Li, M. Liu, C. Jiang, C. Du, Z. Zhao, W. Hu and Z. L. Wang, *Adv. Mater.* **2016**, *28*, 98.
- [22] P.-K. Yang, L. Lin, F. Yi, X. Li, K. C. Pradel, Y. Zi, C.-I. Wu, J.-H. He, Y. Zhang and Z. L. Wang, *Adv. Mater.* **2015**, *27*, 3817.
- [23] J. Wang, X. Li, Y. Zi, S. Wang, Z. Li, L. Zheng, F. Yi, S. Li and Z. L. Wang, *Adv. Mater.* **2015**, *27*, 4830.

- 1
2
3
4
5
6
7
8
9
10
11
12
13
14
15
16
17
18
19
20
21
22
23
24
25
26
27
28
29
30
31
32
33
34
35
36
37
38
39
40
41
42
43
44
45
46
47
48
49
50
51
52
53
54
55
56
57
58
59
60
61
62
63
64
65
- [24] P.-K. Yang, Z.-H. Lin, K. C. Pradel, L. Lin, X. Li, X. Wen, J.-H. He and Z. L. Wang, *ACS Nano* **2015**, *9*, 901.
- [25] T. L. Sun, T. Kurokawa, S. Kuroda, A. B. Ihsan, T. Akasaki, K. Sato, M. A. Haque, T. Nakajima and J. P. Gong, *Nat. Mater.* **2013**, *J2*, 932.
- [26] M. P. Lutolf, *Nat. Mater.* **2009**, *8*, 451.
- [27] E. Calo and V. V. Khutoryanskiy, *Eur. Polym. J.* **2015**, *65*, 252.
- [28] J. P. Gong, Y. Katsuyama, T. Kurokawa and Y. Osada, *Adv. Mater.* **2003**, *J5*, 1155.
- [29] L.-W. Xia, R. Xie, X.-J. Ju, W. Wang, Q. Chen and L.-Y. Chu, *Nat. Commun.* **2013**, *4*, 2226.
- [30] K. Deligkaris, T. S. Tadele, W. Olthuis and A. van den Berg, *Sens. Actuators, 8-Chemical* **2010**, *J47*, 765.
- [31] Y. Xu, Z. Lin, X. Huang, Y. Liu, Y. Huang and X. Duan, *ACS Nano* **2013**, *7*, 4042.
- [32] Z. Chen, J. W. F. To, C. Wang, Z. Lu, N. Liu, A. Chortos, L. Pan, F. Wei, Y. Cui and Z. Bao, *Adv. Energy Mater.* **2014**, *4*, 1400207.
- [33] E. Wang, M. S. Desai and S.-W. Lee, *Nano Lett.* **2013**, *J3*, 2826.
- [34] Q.-F. Li, X. Du, L. Jin, M. Hou, Z. Wang and J. Hao, *J. Mater. Chem. C* **2016**, *4*, 3195.
- [35] S. Wang, L. Lin and Z. L. Wang, *Nano Lett.* **2012**, *J2*, 6339.
- [36] G. Li, H. Zhang, D. Fortin, H. Xia and Y. Zhao, *Langmuir*, **2015**, *31*, 11709-11716.
- [37] R. Ricciardi, F. Auriemma, C. Gaillet, C. De Rosa and F. Laupretre, *Macromolecules* **2004**, *37*, 9510.
- [38] R. Ricciardi, F. Auriemma, C. De Rosa and F. Laupretre, *Macromolecules* **2004**, *37*, 1921.
- [39] S. Niu, Y. Liu, S. Wang, L. Lin, Y. S. Zhou, Y. Hu and Z. L. Wang, *Adv. Mater.* **2013**, *25*, 6184.
- [40] K. Y. Lee, H.-J. Yoon, T. Jiang, X. Wen, W. Seung, S.-W. Kim and Z. L. Wang, *Adv. Energy Mater.* **2016**, *6*, 1502566.

[41] Y. Zi, S. Niu, J. Wang, Z. Wen, W. Tang and Z. L. Wang, *Nat. Commun.* **2015**, *6*, 8376.

[42] E. Chiellini, A. Corti, S. D'Antone and R. Solaro, *Prog. Polym. Sci.* **2003**, *28*, 963.

[43] K. Leja and G. Lewandowicz, *Pol. J. Environ. Stud.* **2010**, *J9*, 255.

[44] F. Abbasi, H. Mirzadeh and A. A. Katbab, *Polym. Int.* **2001**, *50*, 1279-1287.

[45] N. Hallab, K. Merritt, and J. J. Jacobs, *J Bone Joint Surg Am.* **2001**, *83*, 428-428.

1
2
3
4
5
6
7
8
9
10
11
12
13
14
15
16
17
18
19
20
21
22
23
24
25
26
27
28
29
30
31
32
33
34
35
36
37
38
39
40
41
42
43
44
45
46
47
48
49
50
51
52
53
54
55
56
57
58
59
60
61
62
63
64
65

Figure lists

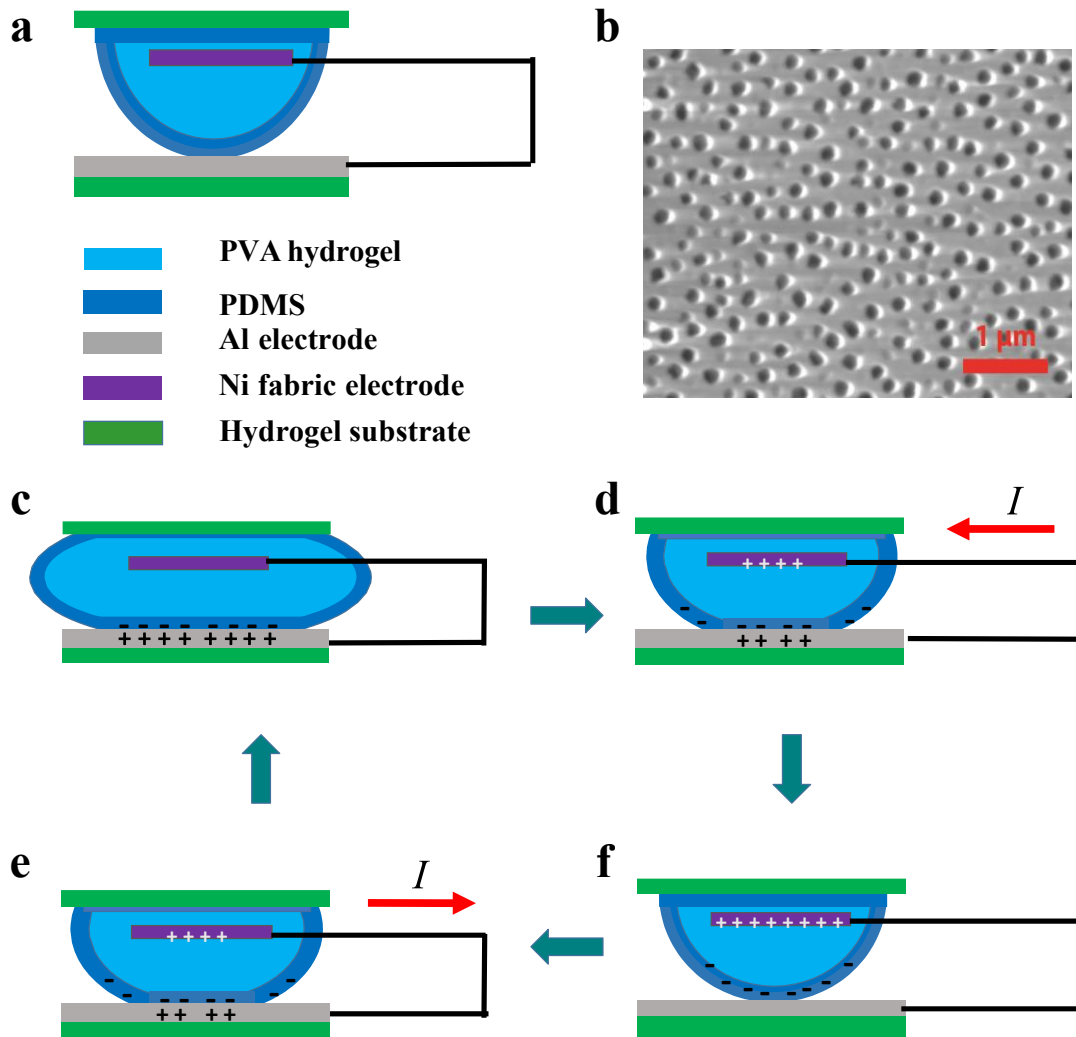


Figure 1. a) Schematic of the standard hydrogel-based triboelectric generator; b) SEM image of Al foil. (c)-(f) Schematic illustration of working mechanism of Hydrogel-TENG. (c) Expanded state (d) Releasing state. (f) Released state. (e). Expanding state.

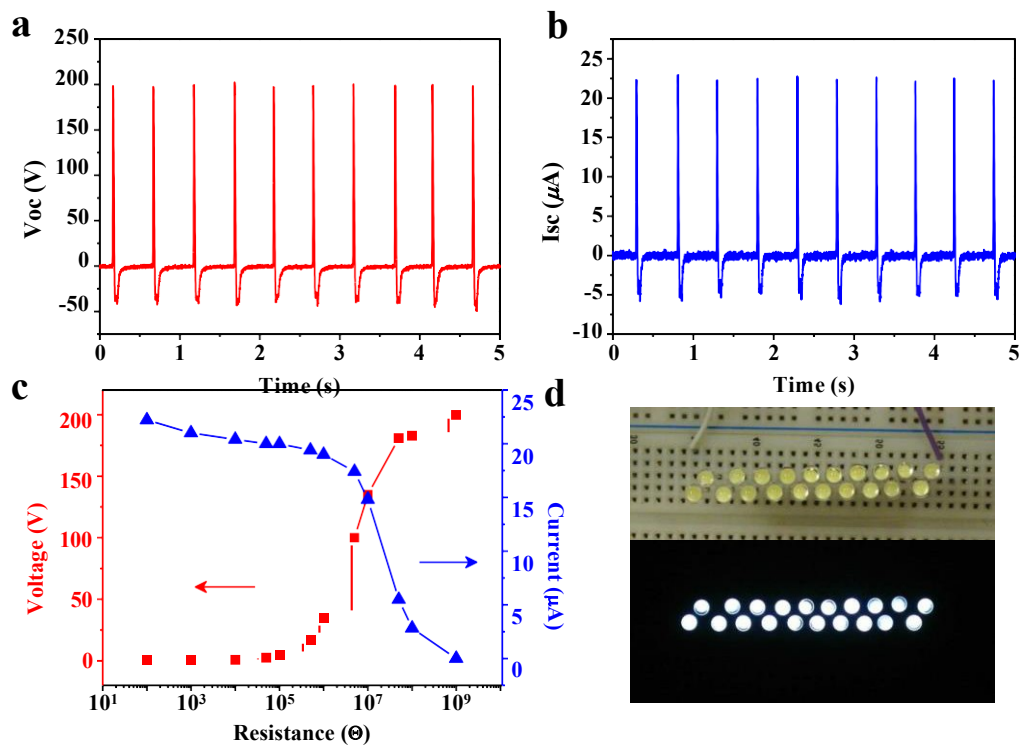


Figure 2. (a) Open-circuit voltages and (b) short-circuit current of the standard Hydrogel-TENG under a frequency of 2 Hz. (c) output voltage and current versus the resistance of the external loads. (d) The optical image of 20 LEDs powered by the standard Hydrogel-TENG.

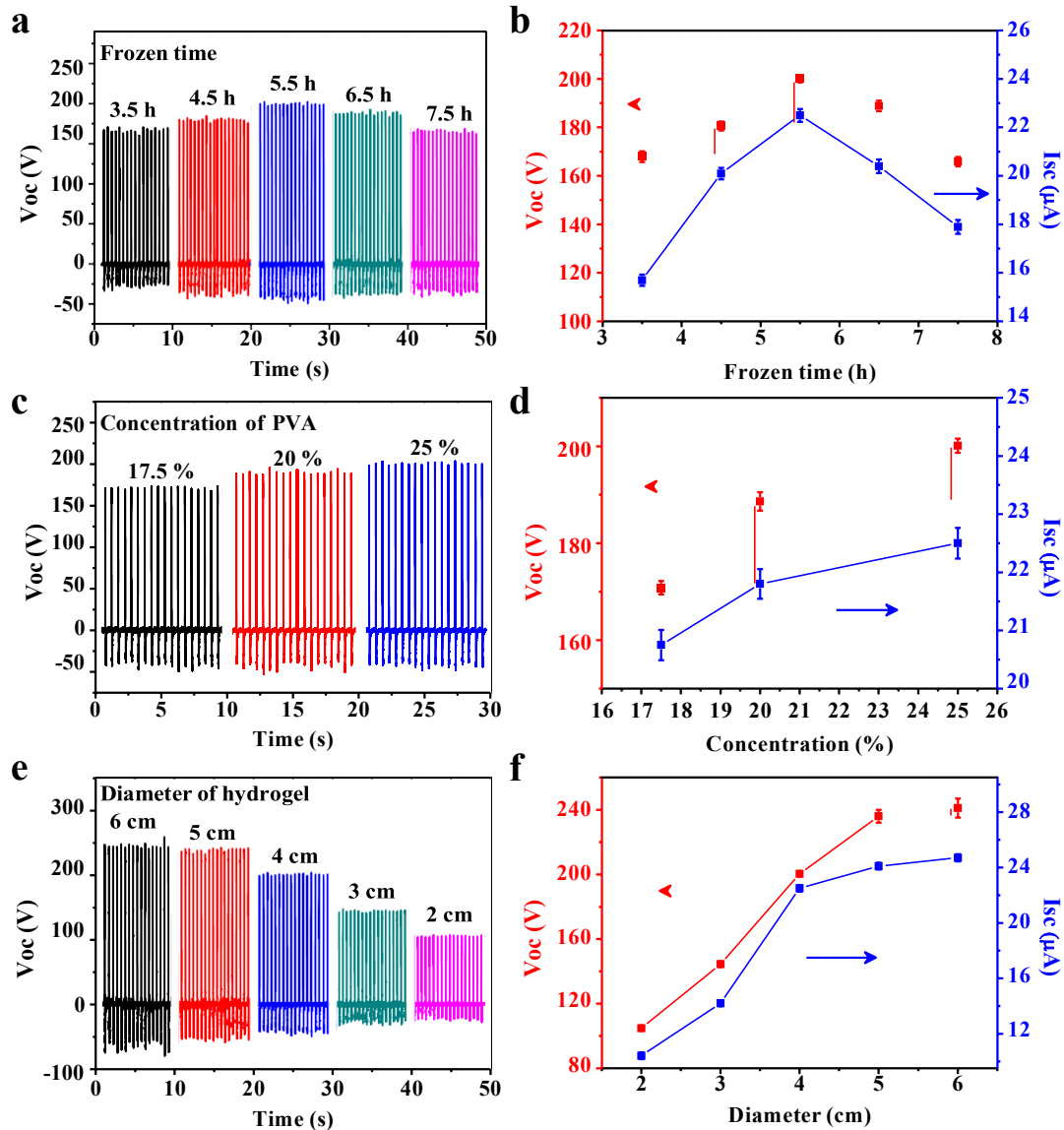


Figure 3. (a) The open-circuit voltage of standard Hydrogel-TENG at different frozen time. (b) The relation between the frozen time and the electric output. (c) The open-circuit voltage of standard Hydrogel-TENG fabricated with the different concentration of PVA. (d) The relation between the concentration of PVA and the electric output. (e) The open-circuit voltage of standard Hydrogel-TENG with the different diameter of hemispheric hydrogel. (f) The relation between the diameter of hydrogel and the electric output.

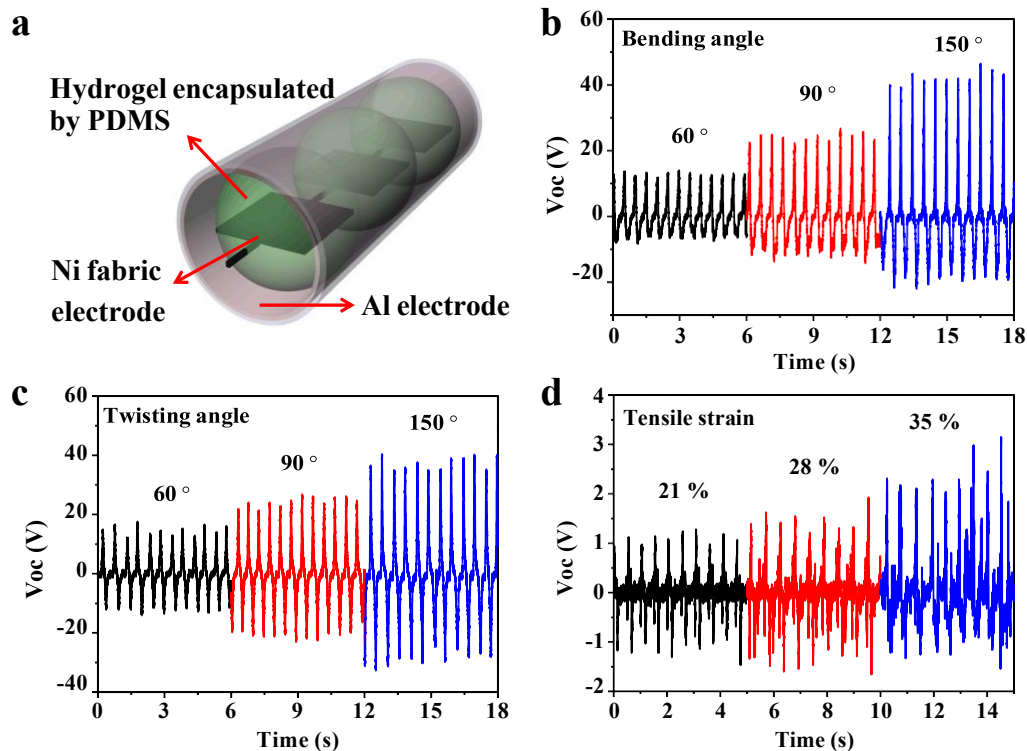


Figure 4. (a) The structural schematic of the tube-shaped Hydrogel-TENG. (b) The open-circuit voltage of tube-shaped Hydrogel-TENG under different bending angel (60° , 90° and 150°). (c) The open-circuit voltage of tube-shaped Hydrogel-TENG under different twisting angle (60° , 90° and 150°). (d) The open-circuit voltage of tube-shaped Hydrogel-TENG under different tensile strain (21 %, 28 % and 35 %).

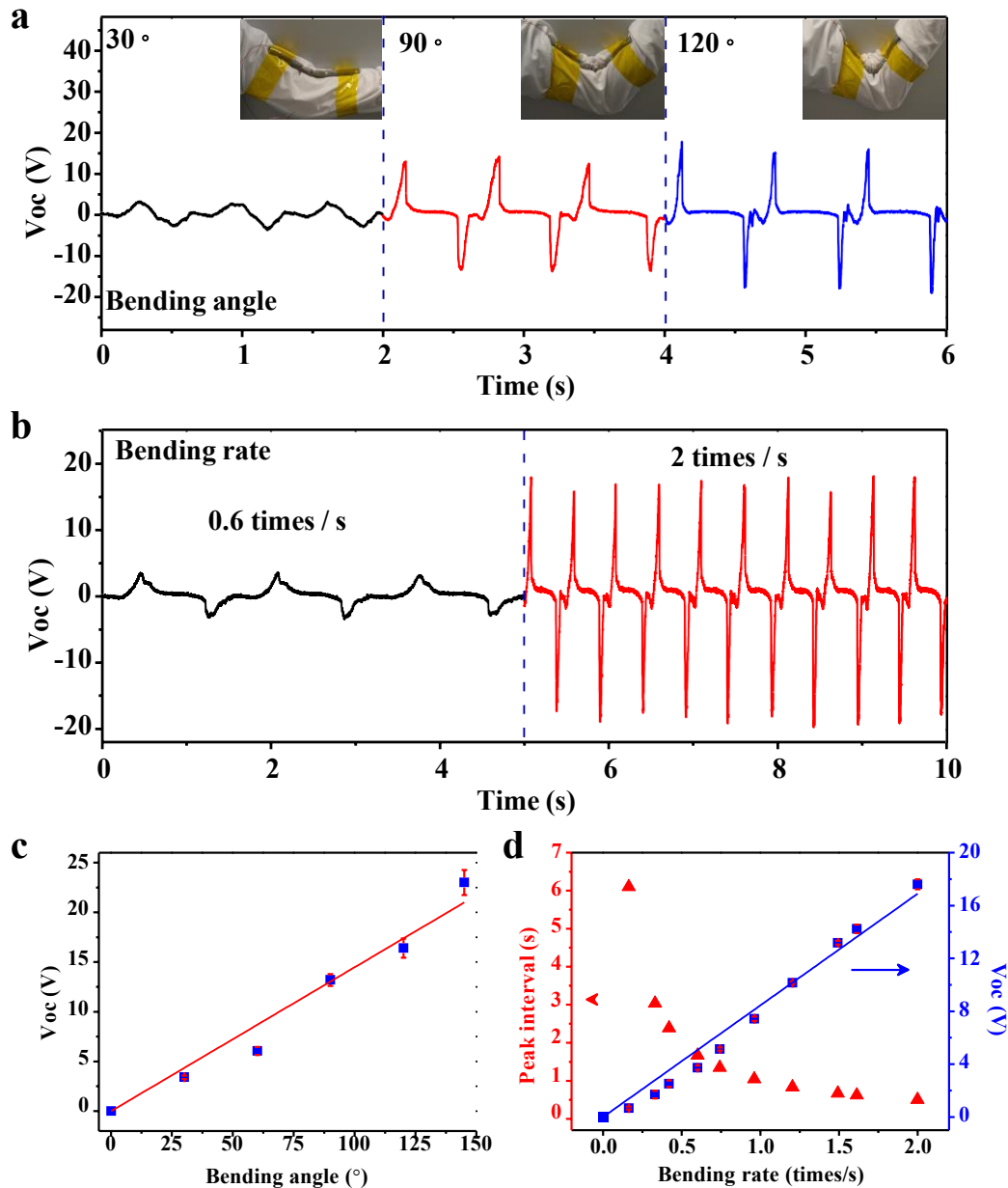


Figure S. Applications of the Hydrogel-TENG to detect joint motion. (a) optical images of the device as the elbow joint motion sensor and the open-circuit voltage responses when bending the elbow joint at different angles (30°, 90° and 120°) (b) open-circuit voltage responses when bending the elbow joint at different bending rates (0.6 times/s and 2 times/s). (c) relationship between open-circuit voltage and bending angle of the elbow joint motion at the bending rate of 1.5 times/s. (d) open-circuit voltage and peak interval versus the bending rate of the elbow joint motion at the bending angle of 90°.

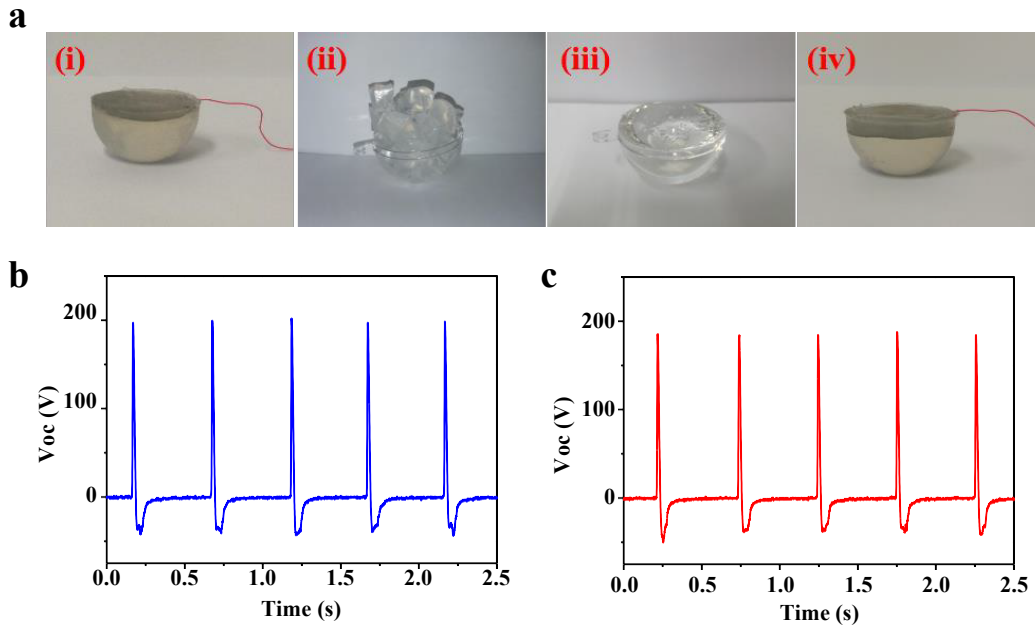


Figure 6. (a) The optical image of the recycling process of PVA hydrogel. (i) The optical image of pristine hemisphere-shaped hydrogel (ii) The optical image of hydrogel pieces. (iii) The optical image of PVA aqueous solution. (iv) The optical image of reshaped hemisphere-shaped hydrogel. (b) The open-circuit voltage of pristine device (c) The open-circuit voltage of reshaped device.

1 **Table of Content:**

2 We firstly demonstrate a hydrogel-based triboelectric nanogenerator with high flexibility,
3 recyclability and environmental friendliness simultaneously for versatile energy harvesting
4 and self-powered human motion sensor. The utilized Polyvinyl Alcohol (PVA) hydrogel is
5 recyclable to benefit for fabricating the renewable TENG, and the Voc of renewed device can
6 reach up to 92 % of the pristine performance.
7

8
9 **Keyword**

10
11
12 Wei Xu, Long-Biao Huang, Man-Chung Wong, Li Chen, Gongxun Bai, Jianhua Hao*

13
14 **Environmentally Friendly Hydrogel-based Triboelectric Nanogenerators for Versatile
15 Energy Harvesting and Self-Powered Sensors**
16

17 ToC figure

